Enhancing Interactive NonPlanar Projections of 3D Geovirtual Environments with Stereoscopic Imaging

Matthias Trapp, Haik Lorenz, Markus Jobst, Jürgen Döllner

Hasso-Plattner-Institut, University Potsdam, Potsdam, Germany

Abstract

Stereo rendering, as an additional visual cue for humans, is an important method to increase the immersion into 3D virtual environments. Stereo pairs synthesized for the left and right eye are displayed in a way that the human visual system interprets as 3D perception. Stereoscopy is an emerging field in cinematography and gaming. While generating stereo images is well known for standard projections, the implementation of stereoscopic viewing for interactive non-planar single-centre projections, such as cylindrical and spherical projections, is still a challenge. This paper presents the results of adapting an existing image-based approach for generating interactive stereoscopic non-planar projections for polygonal scenes on consumer graphics hardware. In particular, it introduces a rendering technique for generating image-based, non-planar stereo pairs within a single rendering pass. Further, this paper presents a comparison between the image-based and a geometry-based approach with respect to selected criteria.

Keywords: Stereoscopic Imaging, Non-planar projections, Real-time rendering

M. Buchroithner (ed.), *True-3D in Cartography: Autostereoscopic and Solid Visualisation of Geodata*, Lecture Notes in Geoinformation and Cartography,
DOI 10.1007/978-3-642-12272-9_20, © Springer-Verlag Berlin Heidelberg 2012

1 Introduction

An increasing number of applications and systems use 3D geovirtual environments (GeoVEs) to integrate, manage, and visualize complex geospatial information. They are typically based on virtual 3D city models and landscape models, which have been standardized by CityGML (Kolbe 2009) recently. Modern geo-media technology, such as cylindrical projection walls or multi-projector non-planar displays (Fig. 1), enables a more intuitive access of geoinformation to broader audiences and for new fields of applications. In contrast to standard 3D applications, their implementation is based on non-planar projection (Trapp, Döllner 2008; Lorenz, Döllner 2008).

As a characteristic feature, geomedia technology provides interactivity, high field-of-view (FOV), and high image resolution, which facilitates the immersion of the user. Further, stereoscopic imaging improves this immersion effect. While planar stereoscopy is well understood and supported by modern rendering systems, stereo rendering under non-planar projections still receives much less attention and rises a number of conceptual and technological challenges, which we would like to address in our contribution.

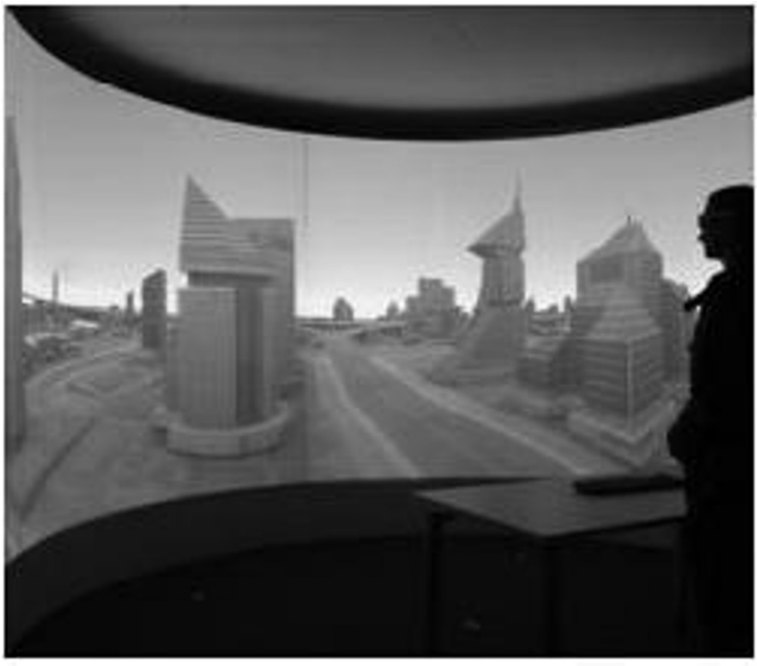

Fig. 1: An example of anaglyph stereorendering under cylindrical non-planar projection demonstrates the usage of 3D stereoscopy in combination with large display technology. (colour version on CD-ROM)

From a cartographic point of view, immersion environments are well-suited as a tool for the effective transmission of complex geoinformation embedded in virtual spaces. Especially psychological depth cues support the intuitive understanding of geoinformation. One main psychological parameter describes the retinal image size. Any restriction of the image size on the retina makes the information transmission less immersive, because any surrounding around the presentation area has an impact on the user's perception. Large projection walls and multi-projector presentation areas enhance retinal image size and, therefore, support psychological depth cues. Non-planar projections together with stereoscopic imaging further improve the degree of immersion.

In this contribution, we discuss with a discussion of the theoretical background of stereoscopic imaging and its application to non-planar projections in the context of cartography and visualization. Next, we present different approaches to interactive stereoscopy rendering techniques for large-scale GeoVE under non-planar projections, including both image-based and geometry-based approaches, which can be implemented on 3D consumer graphics hardware.

We show how these techniques can be applied to passive stereo display techniques, such as anaglyph (Fig. 1 and Fig. 7), polarized, and chroma-depth (Fig. 8), as well as to active stereo display techniques. In addition, we conduct a performance comparison and discuss the respective advantages and disadvantages. The remainder of this paper is structured as follows. Section 2 briefly describes the adaption of two rendering techniques for creating stereoscopic non-planar projections. Section 3 presents application examples of the stereoscopic image-synthesis for 3D geovirtual environments. Finally, Section 4 concludes this work.

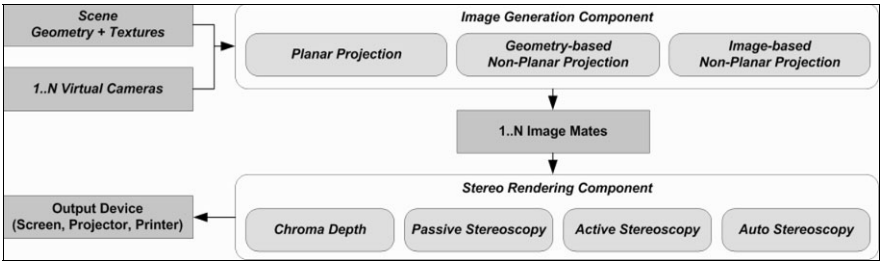

Fig. 2: Conceptual framework for rendering stereoscopic variants of planar and non-planar projections.

2 Stereoscopic Rendering for Non-Planar Projections

This section deals how to adapt existing real-time rendering techniques for non-planar projections to output stereo image pairs. Regardless of the rendering techniques used for creating non-planar projections (NPP), the creation of stereoscopic views comprises the following two basic steps (Fig. 2):

1. **Image Generation**: The NPP for the left and right images are synthesized by using image-based or geometry-based rendering techniques.
2. **Stereo Rendering**: The stereo pairs are combined into a single frame buffer (passive stereo) or rendered into two frame buffer (active stereo) by using post-processing compositing passes.

Besides approaches for omni-directional non-planar projections and camera systems (Peleg et al. 2001) that stitch realworld images to obtain a still stereo image, we find approaches for stereo rendering on multi-projector systems (Bimber et al. 2005). This work reflects non-planar projections for single projection centers which can be created using image-based (IBA) and geometry-based (GBA) approaches. In this work, we focus on the last two.

2.1 Stereoscopic Viewing

To achieve angle and depth disparity that create the stereo effect when viewing, the scene has to be rendered from two virtual eye positions. The eye separation is a distance d in world space. The average distance between the two eyes is $2d = 6.5cm$. Given a virtual reference camera orientation $C = (P, T, U)$, we have to derive the camera settings for the left $C_L = (P_L , T_L , U_L)$ and right eye $C_R = (P_R , T_R , U_R)$. Current applications use three different methods (Bourke, Morse 2007) to obtain these orientations (Fig. 3) by maintaining the up-vector $U = UR = UL$:

- **Parallel Camera Mode:** In parallel mode, the camera position is shifted along the baseline by maintaining the look-to direction $T = T_L = T_R$. The direction of the baseline corresponds to the right vector $R = U \times L$. This results in new orientations for the left camera: $C_L = (P - dR, T_R, U_R)$ and right camera $C_R = (P + dR, T_L, U_L)$.
- **Toe-In Camera Mode:** Additional to the shift of the camera position, the toe-in mode adjusts the look-to vectors with respect to a focal distance d_f. The respective look-to vectors are defined as follows: $T_L = |(P + Td_f) - P_L|$ and $T_R = |(P + Td_f) - P_R|$.
- **Off-Axis Camera Mode:** This mode is similar to the parallel camera mode but uses a non symmetric camera frustum as described in (Bourke, Morse 2007).

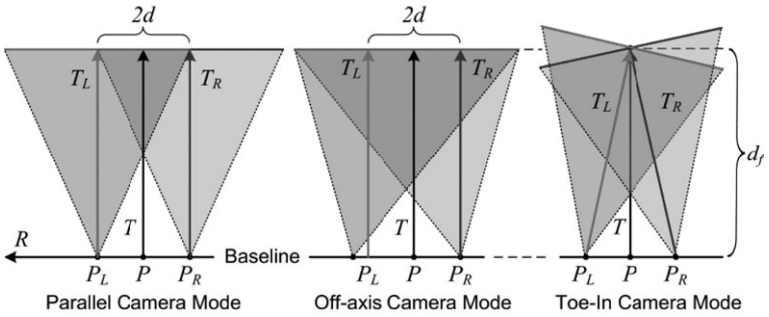

Fig. 3: Comparison of the parameterizations for the parallel, off-axis, and toe-in camera orientation modes for generating stereo pairs. (colour version on CD-ROM)

2.2 Adapting the Imagebased and Geometrybased Approach

These rendering techniques are mainly based on two phases. First, a raster representation of the virtual scene is created using off-screen rendering. In the second phase, this representation is used to create different projections or image distortions using image warping in a post processing step (Yang et al. 2005). In (Trapp, Döllner 2008) a generalization of this approach is described that uses a cube map texture to represent the virtual environment and create multiple NPPs and variants of image distortions. Fig. 4 shows an exemplary rendering pipeline for the image-based creation of two stereo mates. More details of this approach can be found in (Spindler et al. 2006).

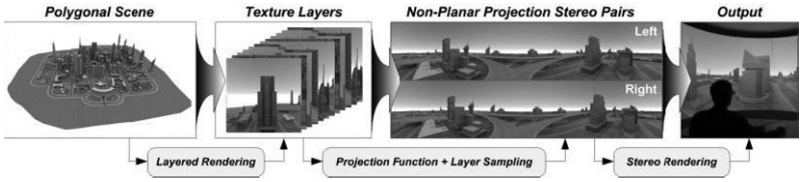

Fig. 4: Pipeline for the stereoscopic rendering of image-based non-planar projections. (colour version on CD-ROM)

A straight-forward GBA implementation simply projects all mesh vertices non-planarly and rasterizes the primitives immediately (Spindler et al. 2006). The inadequate linear interpolation during rasterization requires highly tessellated meshes for artifact-free renderings. Dynamic mesh tessellation based on instancing (Boubekeur, Schlick 2008; Tatarinov 2008), geometry shaders (Lorenz, Döllner 2008), or hardware tessellation units (Tatarchuk 2007) can ensure this property for arbitrary meshes. An alternative approach is tessellating the non-planar projection into smaller and simpler projections. (Hou et al. 2006) describes an approach for rendering arbitrary projections which is conceptually based on beam tracing. In (Lorenz, Döllner 2009), restrict the constituting projections to being perspective. This enables the direct use of GPU rasterization capabilities, but limits the results to single center projections. Based on that technique, Fig. 5 shows an overview how image pairs can be created within a single rendering pass.

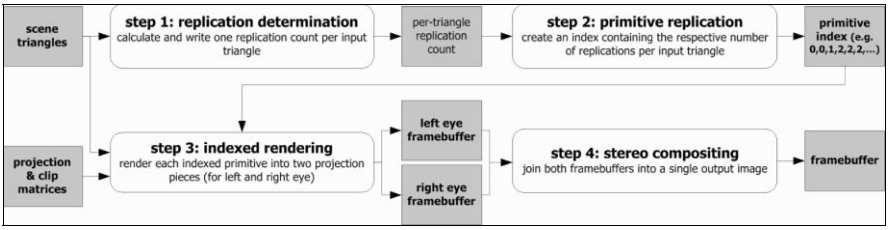

Fig. 5: Adaptation of the geometry-based approach for rendering stereoscopic non-planar projections.

2.3 Comparison

We can compare the geometry-based and image-based approach with respect to the following criteria:

Stereo Functionality

The image-based approach is limited to generating directional panoramic views because the raster representations are created with a fixed base line for each camera orientation. Following to that, the angle disparity is zero for views along the base-line and the user observes only depth disparity. However, the geometry-based approach is able to create full 360° Omni-directional stereo panorama. Further, the GBA is capable of supporting all three camera modes described in Section 2.1 without artifacts. The IBA is limited to the parallel camera mode to avoid artifacts in the stereo pairs. Thus, the GBA has a clear advantage over the IBA.

Rendering Performance

Table 1 shows a comparison between IBA and GBA with respect to the number of input primitives. Both rendering techniques require only a single scene rendering pass for passive stereo viewing of a single cylindrical projection with a horizontal FOV of 180° and a vertical FOV of 90°. The IBA uses cube map face culling to render only necessary faces. The measurement shows that the GBA performs better than the IBA for low to medium model complexity. For a higher model complexity, both approaches obtain similar non-real-time performance but GBA is still faster. In the most common case of rendering a single NPP, GBA should be preferred over the IBA.

Table 1: Performance comparison in frames-per-second (FPS) between the image-based (IBA) and geometry-based (GBA) stereoscopic rendering approaches with respect to the geometric complexity (triangles) of a virtual scene.

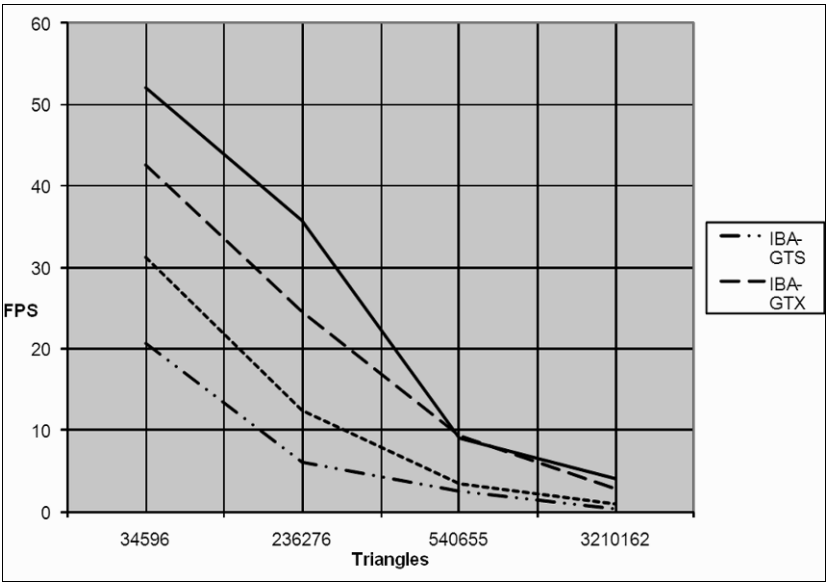

Image Quality

The main drawback of the IBA is image-quality. In contrast to GBA, sampling artifacts are introduced while creating the projections. This is especially problematic for wire-frame renderings or NPR techniques such as hatching or similar ones. Fig. 6 shows the different image quality of both approaches. The quality of the displayed image also depends on the projector systems. However, the GBA is superior over IBA because of its output quality.

Fig. 6: Comparison of the image quality between the geometry-based (left) and image-based approaches (right). The screen shots are conducted using a cube map texture of 2048^2 pixels on a target resolution of 1600 x 1200 pixels. (colour version on CD-ROM)

Memory Footprint

A further criterion considers the memory footprint for data related to the rendering technique, e.g., texture size and geometry. This is an important criterion for applications that use out-of-core rendering mechanisms. The footprint of the IBA can be considered constant. It depends on the texture resolution s, the precision per colour channel b, the number of colour channels c, and the number of raster layers l. The footprint can be approximated by: $O_{IBA}(l,s,b,c) = 2lcbs^2$ byte without mip-maps. This parameterization enables the user to balance the trade-off between image quality and space as well as runtime complexity. Adapting texture resolution according to a projection is problematic, since rasterization speed is optimal for rendering targets sized with power-of-two.

The memory footprint of the GBA is dynamically view depended and scales linearly with the number of input triangles t. Further, memory footprint depends on the average rate of primitive amplification r (for a 180° cylindrical projection $r = 1.5\text{-}2$), and the size of each triangle in an intermediate data structure $i = 16$. The amount of additional memory can be approximated by: $O_{GBA}(t, r, i) = tri$. Following to that, the space complexity of the GBA is independent of rendering a single NPP or a stereo pair of NPP. For the complex model (3,210,162 triangles) the additional memory requirement for a 180° panorama projection is $O_{GBA} \sim$ 69 MB. This corresponds to four RGBA raster layers with 1024^2 pixel resolution. Thus, for a higher FOV: $O_{GBA} < O_{IBA}$ is valid in any case.

Implementation Complexity

This is a subjective criterion and is included for the sake of completeness. Both approaches rely on programmable GPU (geometry shader functionality). The GBA uses transform feedback that is available on current graphics hardware (Blythe 2006). IBA can be considered as easy to implement and integrate into existing rendering frameworks but needs to apply custom cube-map sampling. Since the IBA is independent of the scene geometry, the application of LOD approaches is unproblematic. Further, the application of more complex projections is easy to integrate.

Furthermore, the multi-pass cube map texture creation of the image-based approach provides an implicit fall-back solution for older hardware.

Discussion

The comparison shows that both approaches are capable of rendering stereographic non-planar projections. The GBA is predominant over IBA in the range of functionality with respects to stereo rendering, the quality of the output images, as well as the rendering performance. The IBA has advantages considering the constant space complexity and its implementation. A disadvantage of both rendering techniques is the limitation to polygonal scenes only. They cannot be applied directly to volume rendering without major changes.

Following to these results, we consider the GBA more suitable for stereo rendering of non-planar projections than the IBA. According to our performance measurements, both approaches achieve satisfying results for virtual 3D scenes of the medium complexity of 500,000 triangles. For a scene complexity above this threshold, consumer graphics hardware seems not suitable for stereo visualization.

3 Application Examples

3.1 Active Stereo Rendering

Frame-sequential, active stereo can be achieved by using shutter glasses that are synchronized with the graphics hardware. Here, alternate left and right images are displayed on the screen, multiplexed in time. The user wears LCD shutter glasses which alternately show and hide the left right views. Active stereo can be implemented using OpenGL and a quad buffer (Haines, Akenine-Möller 2002). This feature requires a professional graphics card with hardware stereo support. Similar to polarized rendering, it requires the evaluation of the projection function twice.

Fig. 7: Examples for anaglyph stereoscopic non-planar projections. A: rendering of a horizontal cylinder projection. B: A spherical projection with a field-of-view of 180°. (colour version on CD-ROM)

3.2 Passive Stereo Rendering

Passive stereo viewing is independent of the refresh rates of the output device and can be achieved by using mainly two methods: anaglyph (Fig. 7) or polarized rendering. Anaglyph images provide a stereoscopic 3D effect when viewed with two coloured glasses, each with a chromatically opposite colour (usually red and cyan). The picture contains two differently filtered colour images, one for each eye. This can be implemented by computing two projections and performing a full-screen compositing pass. The image-based approach can be optimized by calculating only a single projection and perform texture sampling from the left and right raster representations. Thus, there is no need to generate stereo pairs. Older anaglyph glasses may introduce problems with reproducing correct colours. Our implementation supports the conversion to gray scale stereo pairs before compositing and the application of a colour optimization scheme as described in (Zhang, McAllister 2006). Another possibility is the use of polarized screens or projector filters in combination with polarized glasses. For the IBA, this approach requires the generation of two projections for the respective buffers.

3.3 ChromaDepth

Stereoscopy

Chromo stereoscopy (Steenblik 1987), or colour stereoscopy, is a three dimensional viewing approach that does not rely entirely on binocular parallax and convergence. This chroma-depth technology is an inexpensive

way to achieve a 3D impression of images that is compatible across different media such as paper or monitor displays. The user needs to wear a chroma-depth glass that performs a colour shift for one-eye. Unlike anaglyph or polarized stereo viewing approaches, the depth perception using chroma-depth glasses relies on colour coding the scene with respect to the current camera settings (Fig. 8). A mapping from the coordinates of a scene point $V = (x, y, z)$ to a normalized colour value C_{out} of the respective chroma-palette has to be computed. The structure of such a function depends on the representation of the colour palette and the mapping of the point coordinates into a palette index. Similar to (Baily, Clark 1998), we represent colour table as 1D texture map. This enables the flexibility to change the colour models, e.g., red-green-blue (RGB), red-white-blue (RWB), or cyan-magenta-yellow (CMY), during runtime. Standardized colour tables can be obtained from the respective vendors of the chroma-glasses.

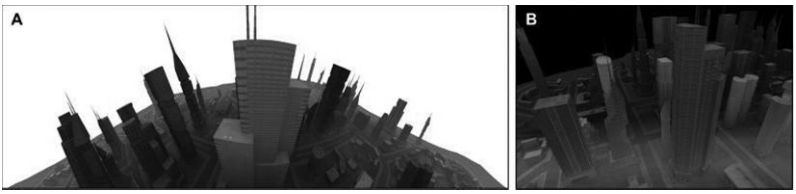

Fig. 8: Examples for chroma-depth stereoscopy: A: A CMY chroma-depth rendering of a horizontal cylinder projection with 360° degree horizontal and 90° vertical field of view. B: A RGB chroma-depth rendering of standard planar projection with 60° field-of-view. (colour version on CD-ROM)

Fig. 9 shows an overview of the components and participating functions of the colour mapping. Given a colour C_{in} obtained by shading and texturing the input scene, the colour palette P as 1D texture, a mixing scalar m, and the eye-space coordinates of a point V, the output colour is obtained by $C_{out} = f_{map}(V, P, m) = f_{lerp}(C_{in}, f_{adjust}(f_{sample}(P, T), m))$. The sampling function f_{sample} performs a texture look-up in P using the generated texture coordinates T. f_{lerp} function performs a linear interpolation between C_{in} and C_C with respect to m. The texture coordinates are obtained by the concatenation of the following 1D functions: $T = f_{rm}(f_{clamp}, f_{dt}(V))$.

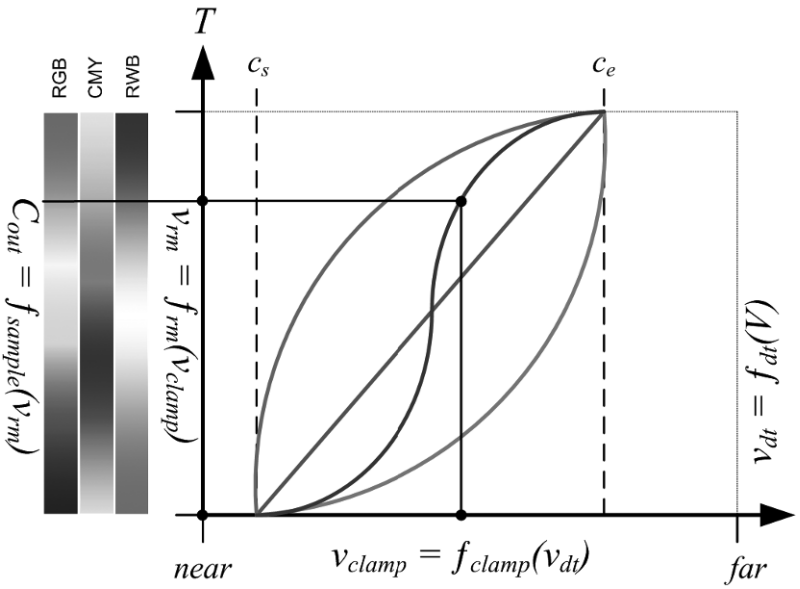

Fig. 9: Components and functions for the chroma-depth colour mapping. (colour version on CD-ROM)

The distance-transform function f_{dt} returns a linear scalar that is clamped and re-normalized using f_{clamp}, and finally re-mapped by f_{rm}. We can parameterize the distance transfer function with respect to the projection that is used. For a standard planar projection, the output equals the value of the z coordinate of V in eye space. For image-based non-planar projections, we set $z = |V_0 - V|$, *i.e.*, the distance of V to the camera position V_0 (Fig. 10).

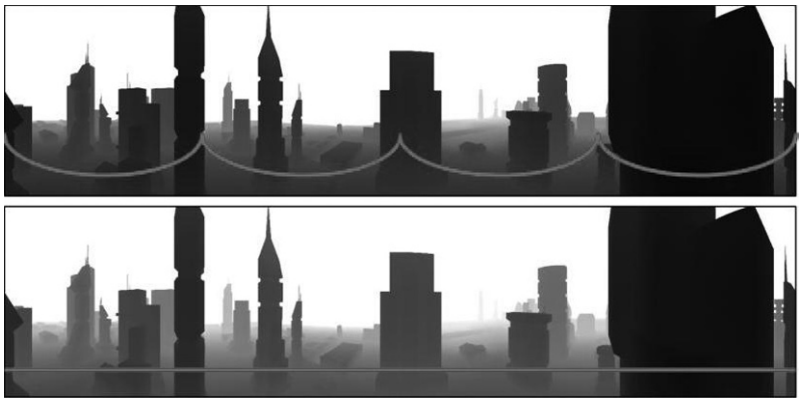

Fig. 10: Comparison of corrected (bottom row) and original (top row) depth values, required to create chroma-depth stereo images using the image-based approach for creating non-planar projections. The line shows the distance between the center of projection of a virtual camera and a single depth complexity. (colour version on CD-ROM)

4 Conclusions

This paper presents an overview for creating stereo renderings of non-planar projections with image-based and geometry-based rendering techniques. In particular, it describes the implementation of a single pass image-based rendering technique as an extension to an existing framework. Further, we describe application examples of stereoscopic rendering to 3D geovirtual environments.

Furthermore, we present a comparison between geometry-based and image-based approaches for generating stereo pairs with respect to four different criteria. This comparison shows that both approaches are capable of rendering stereographic non-planar projections. The GBA is predominant over IBA in the range of functionality with respects to stereo rendering, the quality of the output images, as well as the rendering performance. The IBA has advantages considering the constant space and low implementation complexity. A disadvantage of both rendering techniques is the limitation to polygonal scenes only. They cannot be applied directly to volume rendering without major changes.

Following to these results, we consider the GBA more suitable for stereo rendering of non-planar projections than the IBA. According to our

performance measurements, both approaches achieve satisfying results for 3D scenes of the medium complexity.

References

Baily, M.; Clark, D. (1998) Using ChromaDepth to obtain inexpensive single-image stereovision for scientific visualization. In Journal on Graphic Tools 3, 3 (1998), 1–9.

Bimber, O., Wetzstein, G., Emmerling, A., and Nitschke, C. (2005). Enabling view-dependent stereoscopic projection in real environments. In ISMAR ’05: Proceedings of the 4th IEEE/ACM International Symposium on Mixed and Augmented Reality, pages 14–23,Washington, DC, USA. IEEE Computer Society.

Blythe, D. (2006). The Direct3D 10 System. In SIGGRAPH ’06: ACM SIGGRAPH 2006 Papers, pages 724–734, New York, NY, USA. ACM Press.

Boubekeur, T. and Schlick, C. (2008). A Flexible Kernel for Adaptive Mesh Refinement on GPU. In Computer Graphics Forum, 27(1):102–114.

Bourke, P. D. and Morse, P. (2007). Stereoscopy, theory and practice. Workshop, In VSMM 2007, Brisbane.

Haines, E. and Akenine-Möller, T. (2002). Real-Time Rendering. AK Peters, Ltd., 2nd edition.

Hou, X.; Wei, L.-Y.; Shum, H.-Y.; and Guo, B. (2006). Real-time Multi-Perspective Rendering on Graphics Hardware. In EUROGRAPHICS Symposium on Rendering. Blackwell Publishing.

Kolbe T. H. (2009). Representing and Exchanging 3D City Models with CityGML 3rd International Workshop on 3D Geo-Information, 13.-14. November 2008, Seoul, South Korea. in Lee, Zlatanova (eds.): 3D Geo-Information Sciences, Springer, 2009

Lorenz, H.; Döllner, J. (2008). Dynamic Mesh Refinement on GPU using Geometry Shaders In 16th International Conference in Central Europe on Computer Graphics, Visualization and Computer Vision 2008, February 2008

Lorenz, H.; Döllner, J. (2009) Real-time Piecewise Perspective Projections, In GRAPP 2009 - 4th International Conference on Computer Graphics Theory and Applications, INSTICC Press, pages 147-155, February 2009.

Peleg, S.; Ben-Ezra, M.; and Pritch, Y. (2001). Omnistereo: Panoramic Stereo Imaging. In IEEE Transactions on Pattern Analysis and Machine Intelligence, 23(3):279–290.

Spindler, M.; Bubke, M.; Germer, T.; and Strothotte, T. (2006). Camera Textures. In Proceedings of the 4th GRAPHITE, pages 295–302. ACM.

Steenblik R. A. (1987): The chromostereoscopic process: a novel single image stereoscopic process. In SPIE: True Three-Dimensional Imaging Techniques and Display Technologies, January 1987.

Tatarchuk, N. (2007). Real-Time Tessellation on GPU. In Course 28: Advanced Real-Time Rendering in 3D Graphics and Games. ACM SIGGRAPH 2007.

Trapp M., and Döllner, J. (2008). A Generalization Approach for 3D Viewing Deformations of Single-Center Projections, In GRAPP 2008 - International Conference on Computer Graphics Theory and Applications, INSTICC Press, Number 3, pages 162--170, January 2008

Yang, Y.; Chen, J. X.; and Beheshti, M. (2005) Nonlinear Perspective Projections and Magic Lenses: 3D View Deformation. In IEEE Computer Graphics and Applications, pages 76–84.

Zhang, Z. and McAllister, D. F. (2006). A Uniform Metric for Anaglyph Calculation. In Proceedings Electronic Imaging, San Jose, CA.